

Jan, 13 (1)

A METHOD FOR IN VITRO MAPPING OF ULTRASONIC SPEED AND DENSITY IN BREAST TISSUE

James N. Yang, Anthony D. Murphy, Ernest L. Madsen,<sup>1</sup> James A. Zagzebski,  
Kennedy W. Gilchrist,<sup>2</sup> Gary R. Frank, Michael C. Macdonald, Cameron A. Millard,  
Aviva Faraggi, Carlos A. Jaramillo<sup>3</sup> and Franz R. Gosset<sup>3</sup>

Department of Medical Physics  
1530 Medical Sciences Center  
1300 University Avenue  
University of Wisconsin-Madison  
Madison, WI 53706

<sup>2</sup>Department of Pathology and Human Oncology  
University of Wisconsin-Madison  
K4/550 Clinical Science Center  
Madison, WI 53792

<sup>3</sup>Department of Pathology  
St. Clare Hospital  
Monroe, WI 53566

A method has been developed for mapping density and ultrasonic speed in 1 mm thick slices of soft tissue with a resolution of about 1 mm. Tests using phantom sections have verified the accuracy and resolution of the ultrasonic speed maps. The method has been applied to breast tissues of three patients including tumors and surrounding tissue. Fixing a specimen in 5% formaldehyde did not change the degree of local variation in ultrasonic speeds, and raised mean speeds by less than 0.8%. The densities with fixing remained almost unchanged at low tissue densities (0.93 g/cm<sup>3</sup>), but rose 1.5% for higher tissue density (greater than 1.00 g/cm<sup>3</sup>). © 1991 Academic Press, Inc.

Key words: Breast; density; mapping; speed; tissue; ultrasound.

I. INTRODUCTION

Recognition of echographic patterns in clinical B-mode ultrasound images is one of the most important aspects of diagnostic ultrasound. Variations in ultrasonic speed and density over distances of 1 mm or less are the principal determinants (via scattering) of a tissue's contribution to these patterns. In order to gain quantitative insight into the scattering from within and around tumors it is desirable to determine representative spatial distributions of ultrasonic speeds and densities. This insight could result in increased diagnostic efficacy of scanners if users were led to more intelligent B-mode pattern recognition. Such knowledge may also lead to more realistic simulations of various tissues in phantoms.

<sup>1</sup>Author to whom correspondence should be addressed.

Foster et al. [1] have reported measurements of the ultrasonic speed distribution in 2 mm thick diseased breast tissue specimens using a pulse-echo method with a highly focused transducer operated at 13 MHz. They also investigated the effects on ultrasonic speeds of freezing and thawing the tissue.

Bamber and Bush [2] also described measurements of ultrasonic parameters in breast tissue, including ultrasonic speed but not density. Their tissue slices were 7 mm thick, however, meaning that considerable averaging was done over the 7 mm dimension and that beam distortion effects could be considerable.

In the present work we report on a method for measuring both the ultrasonic speed and mass density distribution in 1 mm thick specimens of breast tissue; also, the ultrasonic speed distributions in two fresh tissue specimens were compared with those after formaldehyde fixing. A through-transmission technique, involving a highly focused source transducer driven with tone bursts at 12.5 MHz and a 0.6 mm diameter receiving hydrophone, was used to measure the ultrasonic speeds. This alternative to the pulse-echo method may offer improved accuracy by reducing phase cancellation effects at reception. Accuracy of these determinations was tested using a test object containing both fat- and nonfat-mimicking material. Density distributions were determined after dicing the tissue specimens into approximately 1 mm<sup>3</sup> pieces, and then applying Archimedes' principle.

Grey-scale images of ultrasonic speed and density are presented in which each pixel corresponds to a 1 mm by 1 mm area on the actual tissue specimens. Values of speed and density tend to be higher within the carcinoma than in its surroundings.

## II. EXPERIMENTAL APPARATUS AND METHOD

### A. Sample preparation

Surgical specimens were obtained either from the University of Wisconsin Hospital in Madison or from St. Clare Hospital in Monroe, Wisconsin. The specimens were analyzed for pathology, placed in a sealed plastic container which was embedded in chipped ice, and then transported by automobile to our laboratory, which is 1.5 miles from the UW Hospital and 50 miles from St. Clare Hospital. The samples arrived within 4 hours of excision. They were immediately attached to a 3 mm thick acrylic plate using DURO super glue [Loctite Corporation, Cleveland, Ohio]. After about 30 minutes, each tissue sample was fast frozen by immersion in a beaker of 2-methylbutane which had been cooled to the temperature of surrounding dry ice (-78°C). Fast freezing was done to minimize microscopic tissue damage due to crystal formation. Subsequently, the specimen was stored at -70°C in a refrigerator until slicing. The storage time usually ranged from 12 to 24 hours. Prior to slicing, the temperature of the specimen was raised from -70°C to -15°C by sealing it in a plastic bag and immersing it in a saline ice bath where the salt concentration was such as to produce a melting point of -15°C. A cryostat maintained at -15°C and containing a microtome blade was used to slice the tissue. In order to diminish effects of variations in ultrasonic speed and density perpendicular to the planar surfaces of the specimens, the slice thickness was kept small (1 mm). Each slice of tissue was then placed over an appropriately sized circular hole in an acrylic frame and glued to the frame at the edges using superglue. The mounted samples were then kept in normal saline at 4°C until measurements were done.

Figure 1 shows a photograph of one of the tissue samples. The diameter of the hole in the frame is 2.8 cm. Dark grey parts of the tissue correspond to

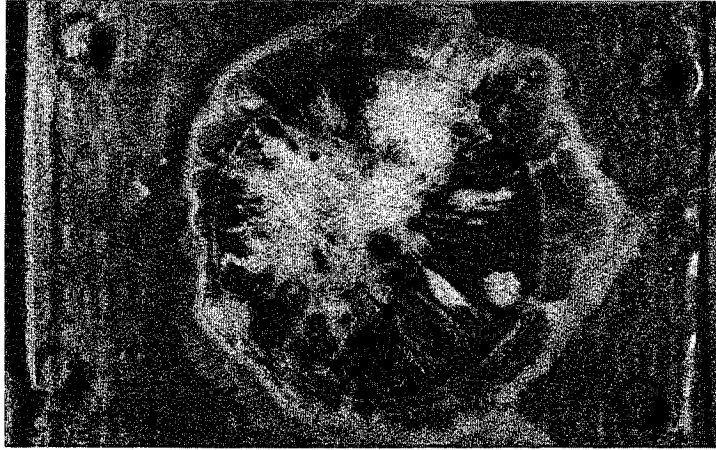


Fig. 1 Photograph of a 1 mm thick slice of tissue including an invasive scirrhous duct carcinoma and surroundings. The sample is attached at its perimeter to an acrylic support with a 2.8 cm diameter hole in it. The tumor is light grey and is centered toward the upper left. Dark grey regions correspond to fatty tissue. Two small dark circles on the tissue, less than 1 mm in diameter, correspond to plastic marker beads. Speed and density maps corresponding to this tissue sample are shown in figure 6.

fatty tissue and light grey to nonfat. The two small dark dots are dyed plastic beads used as markers.

#### B. Ultrasonic speed determination

In the through-transmission technique for determining the ultrasonic speed distribution, the sample is introduced between a source and a receiving transducer, displacing a reference fluid whose speed of sound,  $c_0$ , is known. Measurements of the sample thickness and of the shift in arrival times of the acoustic pulse allow computation of the ultrasonic speed,  $c$ , in the sample using the relation

$$c = c_0 / [1 + c_0 \Delta t / d] \quad (1)$$

where  $d$  is the thickness of the sample,  $\Delta t = t - t_0$  is the difference between arrival times at the receiver with ( $t$ ) and without ( $t_0$ ) the sample in place.

The experimental apparatus is shown in figure 2. The mounted tissue slice was fastened onto a holder which was attached to a set of two cross-mounted micrometers allowing independent vertical and horizontal translations parallel to the planar surfaces of the tissue. The tissue slice was maintained 5.0 cm from a focused 13 mm diameter source transducer with a nominal radius of curvature of 5.0 cm. The nominal frequency of the transducer is 10 MHz, but it was driven with narrow band bursts at 12.5 MHz. The full width at half maximum (FWHM) amplitude at 5 cm from the transducer is 0.83 mm as determined from a plot of the lateral beam profile at 5.0 cm from the source. A 0.6 mm diameter PVFD hydrophone [Medicoteknisk Institute, Copenhagen, Denmark] was used in obtaining this beam profile, no correction being attempted to account for the

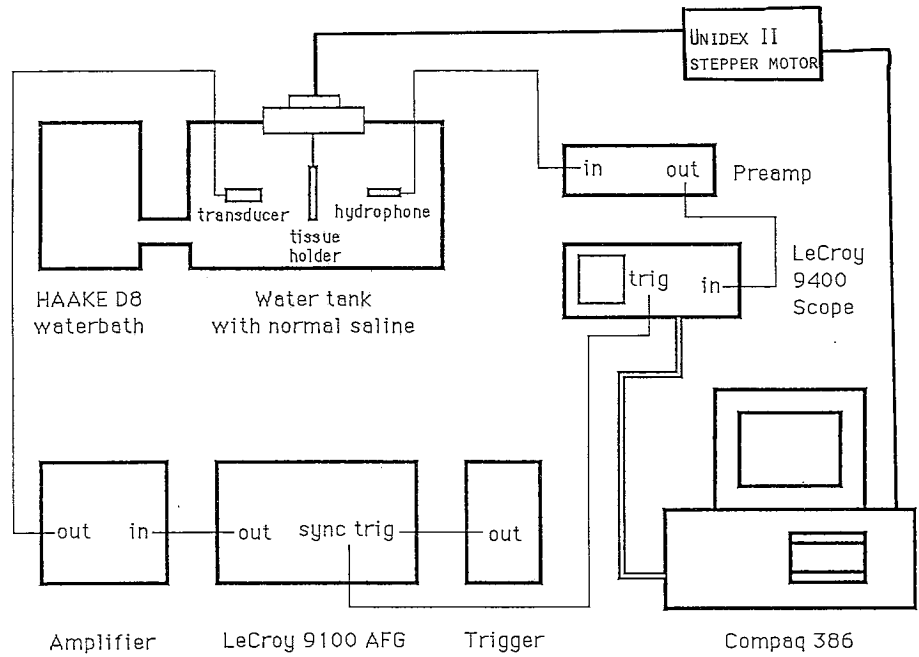


Fig. 2 Schematic diagram of the experimental system used in ultrasonic speed determinations.

fact that the FWHM found was comparable to the diameter of the receiving element. This same hydrophone was used to receive the transmitted pulses, the receiving element being placed 5 cm distal to the tissue specimen (in the far field) where the beam diameter was about 1 cm. The small receiving area of the hydrophone minimized phase cancellation effects at the receiver related to beam distortions which might occur when the incident beam passed through the tissue specimen.

The water tank was filled with normal saline as the reference fluid. The temperature of the saline was monitored with a Taylor Permafused thermometer (25°C to 55°C range) calibrated at the National Bureau of Standards; according to the calibration report received at the time of purchase of the thermometer, at the NBS standard reading of 35.000°C this thermometer also read 35.000°C. We estimated our uncertainty reading the thermometer to be 0.05°C. The temperature of the water bath was kept constant at 37.00 ± 0.05°C by a Haake D8 constant temperature water bath [Haake-Buchler Instruments, inc., Saddle Brook, NJ]. The constant temperature water bath was external to the water tank containing the tissue sample, fluid exchange being accomplished with the pumping system of the former and three large bore return siphons. To achieve the high degree of thermal stability (± 0.05°C) in the water tank, it was insulated thermally by covering the sides with 2.5 cm thick polyfoam and covering the upper surface of the circulating saline with polyfoam "popcorn" of the type used in packaging.

This temperature stability means that variations of the ultrasonic speed in the saline due to fluctuations in temperature were less than about ± 0.2 m/s. The speed of sound in the saline, measured with a standard method [3] at 37.00°C, was 1534.2 m/s.

MAPPING OF ULTRASONIC SPEED AND DENSITY

Pulse bursts of 12.5 MHz were produced by a LeCroy 9100 arbitrary function generator, amplified, and applied to the source transducer. The hydrophone signal was sent to a preamplifier and then to a LeCroy 9400 digital oscilloscope. The value of  $\Delta t$  was determined by recording the time shift on the scope corresponding to a specific zero crossing in the received signals. To insure that the same zero crossing was always monitored, a section of the sinusoidal burst was "tagged" using the arbitrary function generator by increasing the amplitude of a specific cycle by 20% relative to the adjacent cycles in the burst. The zero crossing monitored was chosen sufficiently near the beginning of the pulse that reverberations within the sample were avoided.

To observe the variations in ultrasonic speed in such thin samples, it is necessary to measure  $\Delta t$  very accurately. To achieve the required accuracy, a computer controlled data acquisition system was used with a GPIB IEEE-488 instrumentation interface [National Instruments Corporation, Austin, Texas] connecting the digital oscilloscope to the host computer. The sampling rate of the oscilloscope in its "random interleaved sampling mode" is 5 GHz [4]. (Note: This mode assumes a repetitive signal; the actual "one shot" sampling rate is 100 MHz.) At least two waveforms were recorded and averaged for each time of flight to enhance precision. The zero crossing time was obtained by interpolating, assuming linearity between voltage and time exists within 1 digitized voltage level of the zero voltage. (There are 256 levels in all.)

A raster scan was performed in which the specimen was translated in 1 mm steps between temporal data acquisitions. The scanned areas depend on the size of the tissue specimens; for two of the samples reported the area was 20 mm by 20 mm. Data for all 400 positions were usually acquired in about 90 minutes. For another set of samples corresponding to the region of a specific tumor in a different patient, the scanned area was an 18 mm diameter circle.

The uncertainty in ultrasonic speeds is given by

$$\sigma = [(\partial c/\partial d)^2(\sigma_d)^2 + (\partial c/\partial t)^2(\sigma_t)^2 + (\partial c/\partial t_0)^2\sigma_{t_0}^2 + (\partial c/\partial c_0)^2(\sigma_{c_0})^2]^{1/2} \quad (2)$$

where  $\sigma_d$  is the uncertainty in sample thickness, etc. The uncertainties of a single measurement of  $t$  and of  $t_0$  are 0.7 ns, and the uncertainty in the reference ultrasonic speed is 0.5 m/s. The uncertainty of  $t$  or  $t_0$  was estimated experimentally to be the standard deviation of a set of 20 successive measurements corresponding to independently obtained waveforms in which no change in the experimental setup occurred; thus, jitter in trigger-pulse synchronization was accounted for. The thickness uncertainty, which conservatively is about 0.1 mm, was assessed using ultrasonic pulse-echo methods and direct micrometer measurements. Analysis of Eq. (2) with the above contributing uncertainties shows that  $\sigma$  is determined almost entirely by  $\sigma_t$ ,  $\sigma_{t_0}$  and  $\sigma_d$  and that variation in  $\sigma$  with  $c$ , over the range of  $c$  involved, depends on  $\sigma_d$  (see Appendix). In figure 3 are shown  $\sigma$  plotted versus  $c$  (solid line) and the value  $\sigma$  would have if  $\sigma_d$  were zero (dashed line). The uncertainty in  $c$  ranges from about 2 m/s where  $c \approx c_0$  to 12 m/s at  $c \approx 1400$  m/s. Notice that outside of the range  $1520 \text{ m/s} < c < 1560 \text{ m/s}$ ,  $\sigma$  varies approximately linearly in  $c - c_0$ ; this linear behavior is related to thickness uncertainty.

An experimental test of the accuracy of this system was done using a sample slice composed of tissue-mimicking (TM) ultrasonic phantom materials. (See Results and Discussion section.) The sample was a 2.5 cm diameter disc with a thickness of 1.5 mm. Most of the sample was agar gel containing 4.5 percent dry weight Difco Bacto agar (Difco Laboratories, Detroit, Michigan). Near the center of the disc was a fat-mimicking section composed of an oil-in-agar gel dispersion, produced following techniques described in an earlier paper [3].

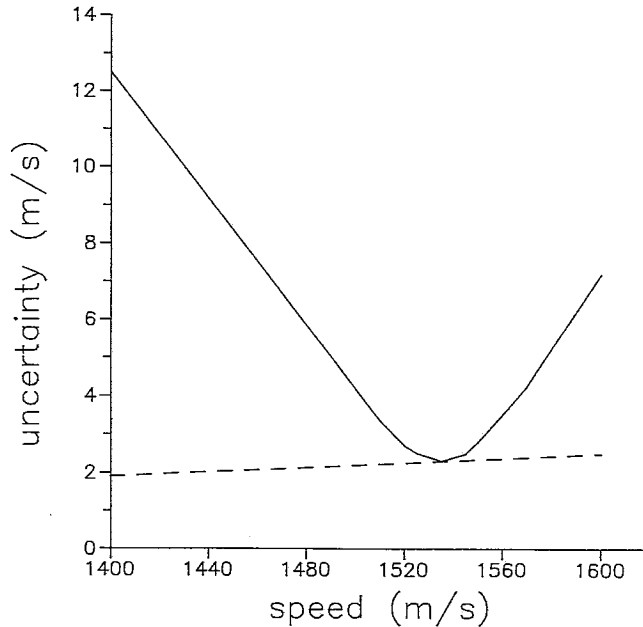


Fig. 3 Uncertainty in measurements of ultrasonic speeds as a function of measured speed. The solid line is the total uncertainty, and the dashed line is that without accounting for sample thickness uncertainty.

This section consisted of a slice including the center of a 6.3 mm diameter sphere.

At the time of production of each material used in making the test disc, two cylinders, with diameters of 7.6 cm and thicknesses 5.0 cm, were produced for use in making accurate measurements of their ultrasonic speeds. Measurements on these large samples were made using methods described earlier [3]. The resultant values of the speed at 37.0°C were  $1535.1 \pm 0.5$  m/s for the agar and  $1469.6 \pm 0.5$  m/s.

#### C. Density determination

Density measurements were carried out on small pieces of tissue using Archimedes' principle. First the 20 mm by 20 mm section of the tissue specimen on which ultrasonic speeds had been measured was diced into 400 pieces, each approximately a  $1 \text{ mm}^3$  cube. The relative positions of the pieces in the original sample were maintained by placing each piece in the appropriate one of 400 hemispherical depressions arranged in a 20 by 20 square array on an acrylic plate. In addition to the small piece of tissue, each depression contained a drop of normal saline to prevent desiccation. The density of each piece was determined by placing it into one or more of a set of solutions of a 14-carbon chlorinated hydrocarbon [Trade name: Chlorowax, Occidental Chemical Corporation, Dallas, Texas] and n-tetradecane. Thirteen solutions were used, having specific gravities of 0.920, 0.940, 0.960, 0.980, 1.000, 1.010, 1.020, 1.030, 1.040, 1.050, 1.060, 1.070 and 1.080. If the piece neither sank nor rose in a solution, then the density of the piece was taken to be that of the solution.

If the piece rose in one solution and sank at a comparable rate in the solution with a next lower density, then its density was taken to be the average of those two solutions. The largest increment in density is  $0.020 \text{ g/cm}^3$ . Using the technique described, the density uncertainty is then  $\pm 0.005 \text{ g/cm}^3$  assuming the solution densities are accurate and that the technique is valid for deciding that the sample density is best approximated as the average of two solution densities.

The densities of the solutions themselves were monitored using precision hydrometers [Fisher Scientific Company, Pittsburgh, Pennsylvania], and the uncertainty in the tissue densities determined is estimated to be  $\pm 0.006 \text{ g/cm}^3$  using the following error analysis. The uncertainty in the solution densities were estimated to be  $\pm 0.0025 \text{ g/cm}^3$  based on the following facts: 1) The densities of the solutions were measured before and after density measurements on a tissue slice, and a change of more than  $0.002 \text{ g/cm}^3$  in solution density was never observed. 2) The densities before measurements were always within  $0.001 \text{ g/cm}^3$  of the specified value; e.g., the  $0.900 \text{ g/cm}^3$  solution was always between  $0.899$  and  $0.901 \text{ g/cm}^3$  according to the hydrometer. 3) The hydrometers are certified by the manufacturer, using NBS standards, to be accurate within one division ( $0.001 \text{ g/cm}^3$ ) at  $20^\circ\text{C}$  which is within  $1^\circ\text{C}$  of the temperature of measurement. Thus, propagation of errors yields an estimated uncertainty of the actual liquid densities of  $\pm [ (0.002)^2 + (0.001)^2 + (0.001)^2 ]^{1/2} = \pm 0.0025 \text{ g/cm}^3$ . Regarding the measurements on the tissue samples, themselves, the procedure described above implies an error of  $\pm 0.005 \text{ g/cm}^3$ . If the uncertainties in the densities of the two reference solutions included, the total propagated error becomes

$$\pm [ (0.005)^2 + (0.0025)^2 + (0.0025)^2 ]^{1/2} = \pm 0.006 \text{ g/cm}^3.$$

It is important to use water-immiscible solutions, composed of large molecules, in order to measure the densities correctly. Since water is a dominant component of most tissues, the suspending solution will not enter the tissue specimen and change its density during measurement. Even for pieces of adipose tissue, diffusion of the large 14 carbon molecules through cell membranes was unlikely during the short measurement period; regarding testing the latter idea, the measured densities of adipose tissue specimens were found to remain unchanged over a period of 10 minutes in solution.

Specially designed transparent acrylic miniature dunking buckets with a removable stainless steel screen on each end were used to enhance efficiency of density determinations. Without these buckets, retrieval of the piece from the solution could be time consuming. After removing excess liquid using a Kimwipe paper absorber [Kimberly-Clark Corporation, Rosewell, GA], a piece of tissue was loaded into a bucket and then immersed into one of the solutions. Before immersion in the next solution, most of the former solution was removed by touching the bucket on a Kimwipe. The density of a piece was usually determined after immersion in 2 or 3 solutions. Two persons can make 400 measurements in about 5 hours. However, dicing a 1 mm thick 20 mm by 20 mm tissue specimen into 400  $1 \text{ mm}^3$  pieces demands about the same amount of time. If a third person dices the specimen while the other two do density measurements, the total time for 400 measurement remains about 5 hours.

## V. RESULTS AND DISCUSSION

A diagram showing the phantom geometry is shown in figure 4a, and in figure 4b is shown a grey-scale map of ultrasonic speeds in the phantom disc on a field of 10 mm by 10 mm. Note that in this case the translation between adjacent mapping points was 0.5 mm instead of 1.0 mm. A histogram showing the

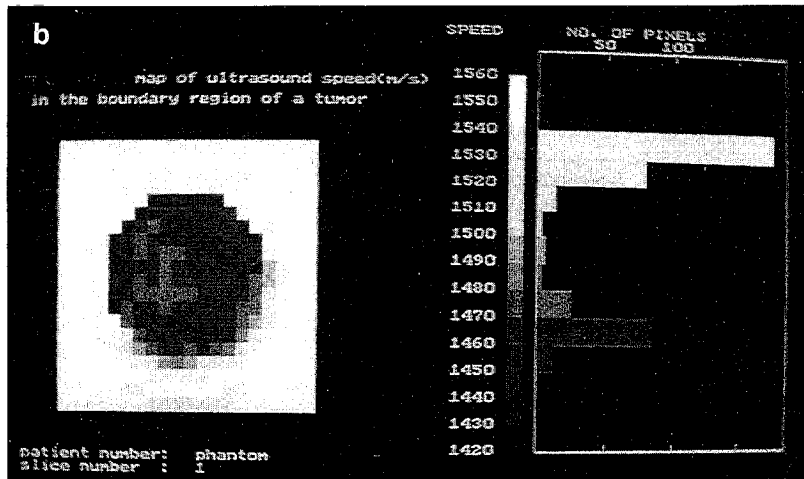
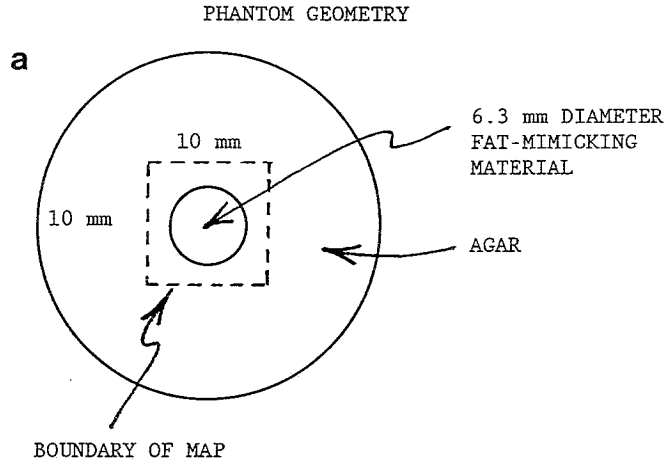


Fig. 4 (a) Diagram showing the geometry of the test phantom formed from tissue-mimicking material which includes a 6.3 mm diameter disc of fat-mimicking material near the center. (b) Ultrasonic speed mapping of a 10 mm by 10 mm field centered on the fat-mimicking disc of the test phantom. The raster scan was done in 0.5 mm steps. On the right is a histogram of the ultrasonic speeds.

distribution of measured ultrasonic speeds is shown on the right of the figure. The mean ultrasonic speed and standard deviation of the ultrasonic speeds in the pure agar region outside the fat-mimicking disc are 1532.2 m/s and 2.3 m/s, respectively; the corresponding values inside the fat disc are 1467.7 m/s and 2.6 m/s. The mean values are in good agreement with the values of 1535.1 m/s and 1469.6 m/s obtained using larger samples of the two types of materials. The mapping depicts the fat-mimicking disc rather well. The diameter of the disc on the map appears to be close to the actual 6.3 mm diameter of the fat-mimicking disc. However, at the boundary between the fat-mimicking material and the plain agar, there are some dramatic changes in measured speed. This probably results from distortions in the beam due to the large variations in speed and, perhaps,



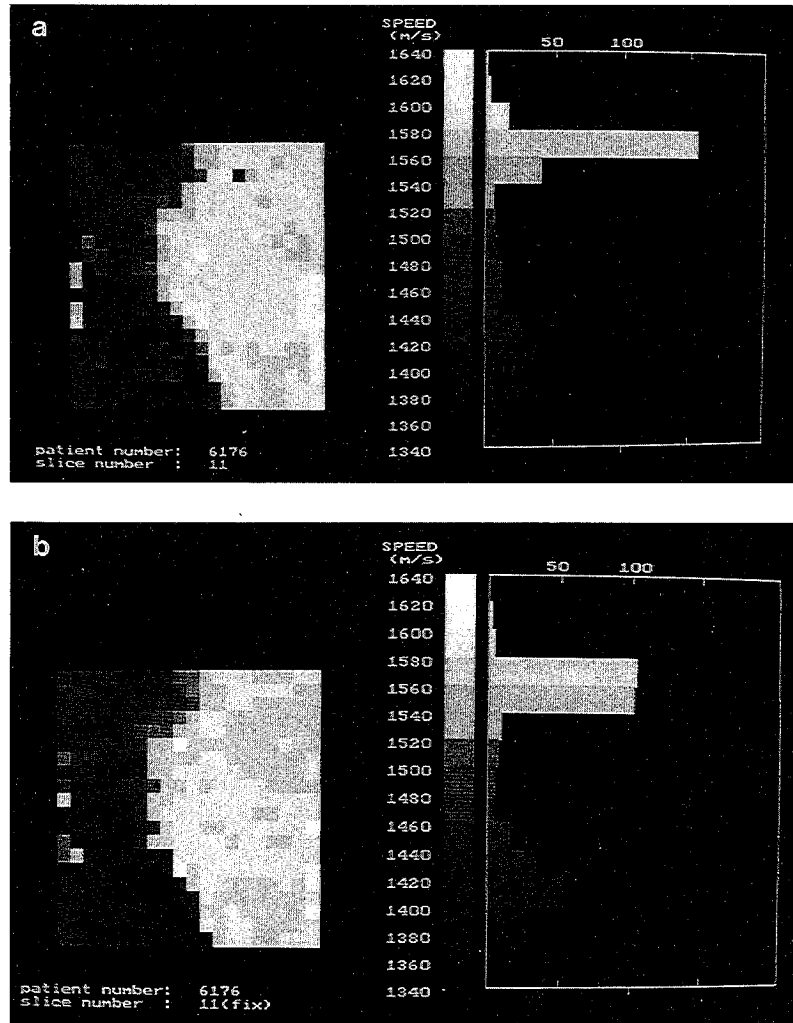


Fig. 5 Mappings of ultrasonic parameters over a 1 mm thick slice of breast tissue in the region of an infiltrating adenocarcinoma: a) ultrasonic speed in the fresh specimen; b) speed after 3 days fixing in 2% formaldehyde (by weight); c) density in fixed tissue; d) acoustic impedance map.

density. Thus, the mapped ultrasonic speeds at the boundary between two materials of very different ultrasonic properties were not very accurate. From figure 4b, the resolution of the ultrasonic speed mapping was estimated to be about 1 mm.

The results for tissue samples are displayed in figures 5-7 and tables 1-3. In figures 5 and 6 are shown grey scale maps of ultrasonic speed and density — or functions of these variables — for two diseased breast tissue samples, each from a different patient. In tables 1 and 2 are shown means and standard deviations of ultrasonic speed measurements for regions of the two tissue

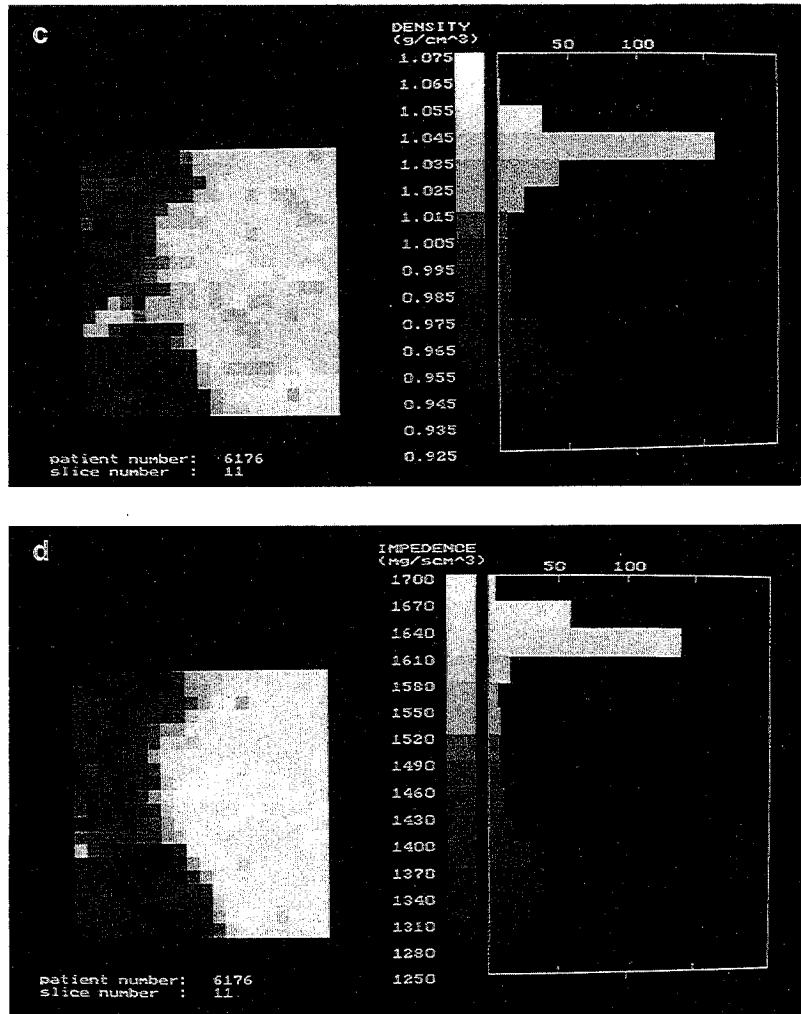


Fig. 5 Continued

samples either inside or outside the apparent tumor boundary. Figure 7 shows a sequence of eight speed and density maps corresponding to successive slices through a third diseased specimen. In table 3 are shown densities of randomly selected pieces of tissue before and after formalin fixing.

Figures 5a-d correspond to a single slice through an infiltrating adenocarcinoma from a 51 year old patient. The main body of the tumor was firm (not maleable) and also uniform in appearance to the naked eye. The cancer occupies approximately the right half of the maps, and fatty surroundings occupy the remainder. Figure 5a shows the ultrasonic speed mapping and a histogram of the speeds for the fresh specimen. The mean and standard deviation of the speed values within different regions of the specimen are shown in the left column of table 1. Values for these tissues are consistent with values obtained previously via *in vivo* ultrasound computerized tomography by Greenleaf and Bahn

MAPPING OF ULTRASONIC SPEED AND DENSITY

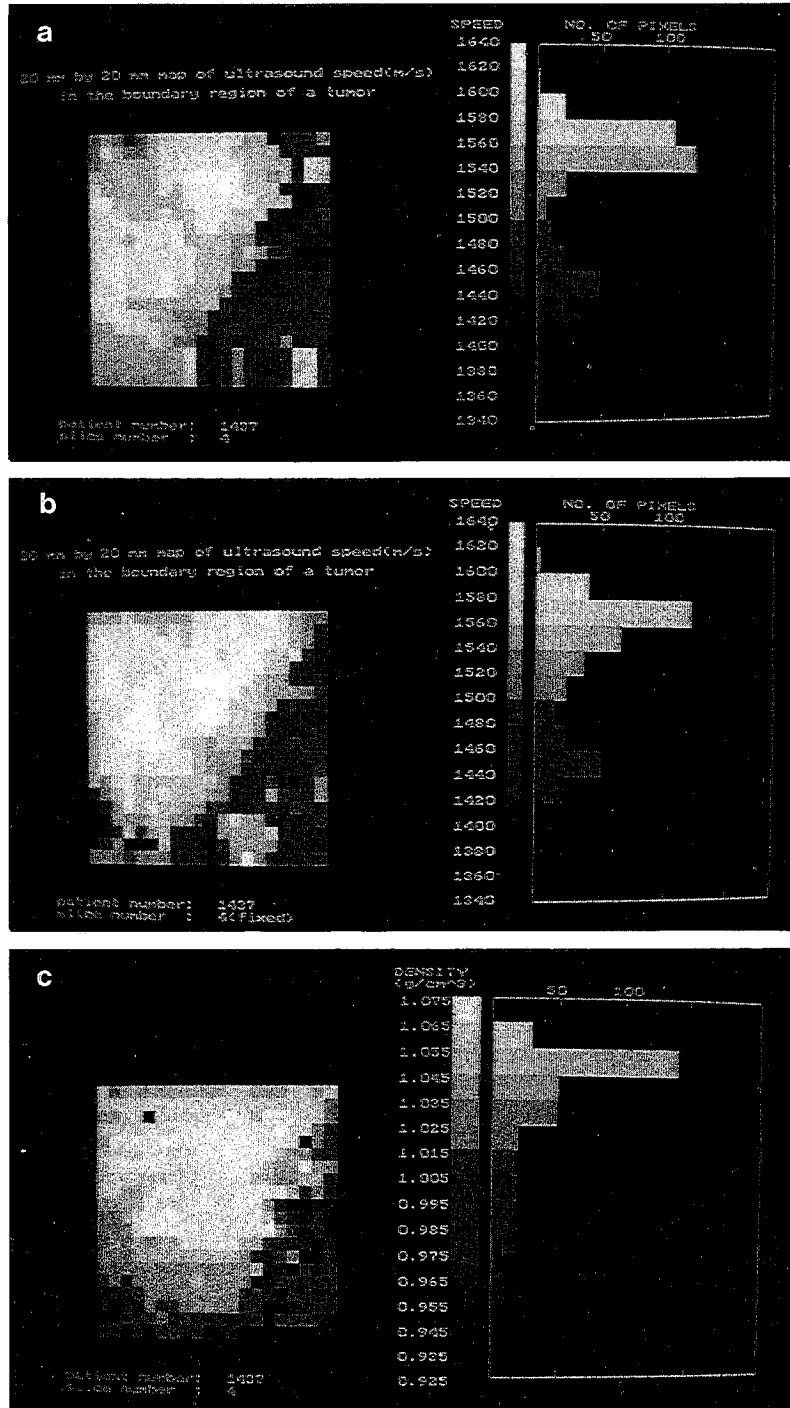


Fig. 6 Mappings of ultrasonic parameters over a 1 mm thick slice of breast tissue in the region of an invasive scirrhous duct cell carcinoma: a) ultrasonic speed in the fresh specimen; b) speed after 1.5 days fixing in 5% formaldehyde (by weight); c) density in fixed tissue.

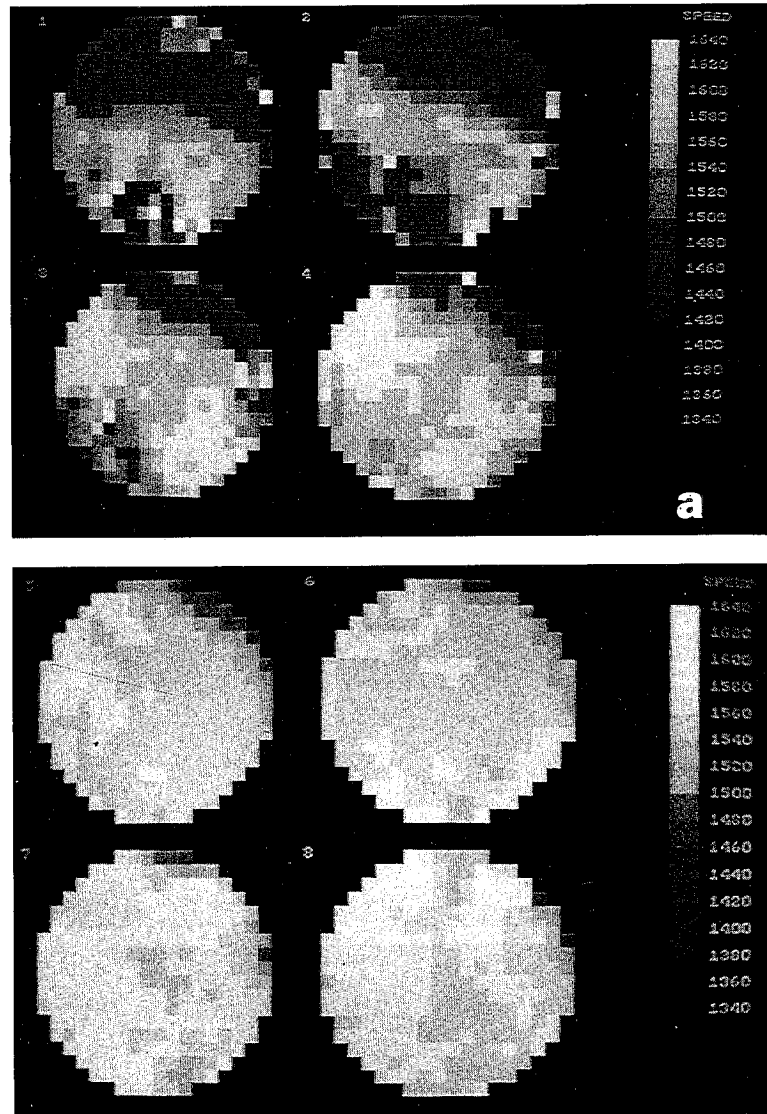


Fig. 7 Mapping of ultrasonic properties in eight successive fresh tissue slices through the duct cell carcinoma of a third patient. The slicers are numbered in order. a) ultrasonic speed; b) density.

[5]. They found that fibrous carcinomas tend to have ultrasonic speeds between 1530 m/s and 1580 m/s, and breast fat in the region of parenchymal tissue has speeds in the range of 1400 m/s.

In figure 5b is shown an ultrasonic speed map of the same sample after storing 3 days in normal saline at room temperature containing 2% by weight HCHO (formaldehyde). As shown in column 2 of table 1, the mean speed in the tumor decreased by 8 m/s with formalin fixing and the mean speed in the surrounding

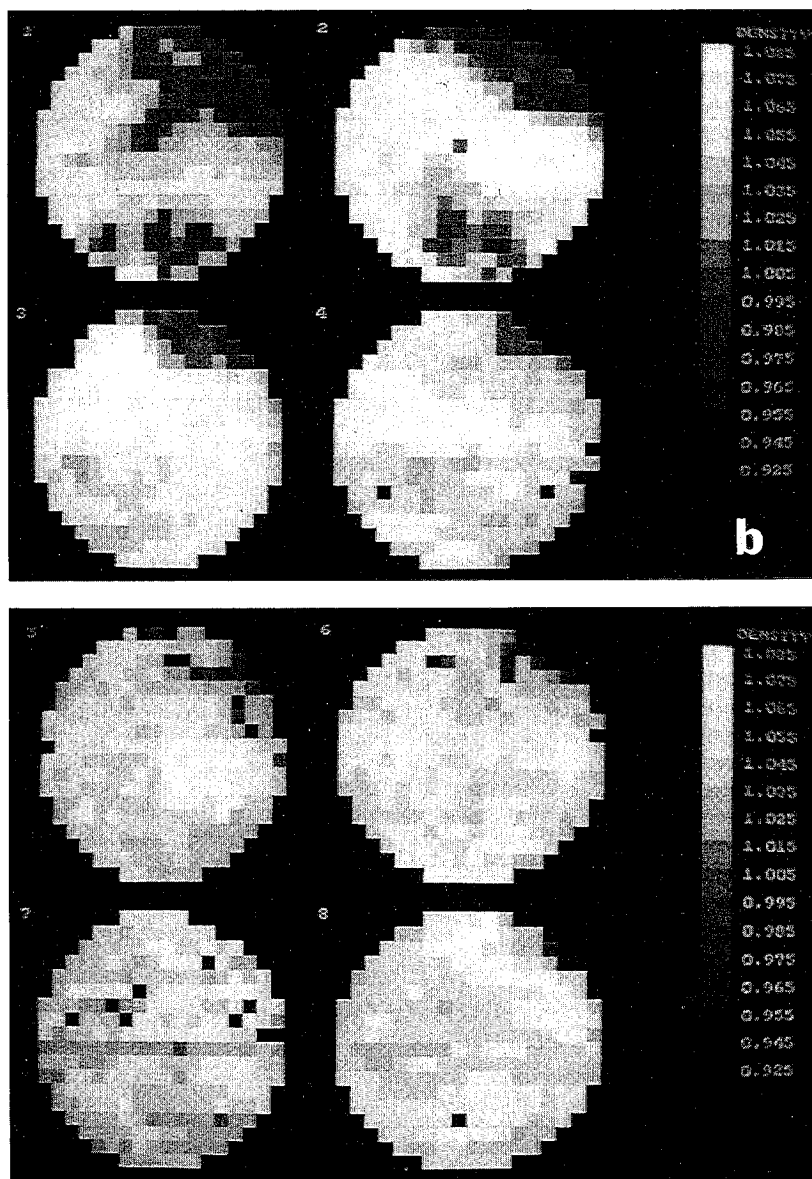


Fig. 7 Continued

(fat) increased slightly by 2 m/s. The standard deviation decreased by about 17% in both the carcinoma and the fatty surroundings. Thus, the ultrasonic speeds became more homogeneous with formalin fixing. The greater homogeneity also is apparent in the mappings themselves in figures 5a and 5b, particularly in the fatty region.

In figure 5c is shown the density mapping for this tissue slice with the histogram of values on the right. The density in the tumor has a mean and

Table 1. Statistics for speed distributions shown in figures 5a and 5b.

	fresh specimen	fixed specimen (2% HCHO)	fixed value minus fresh value
mean speed in tumor (m/s)	1567	1559	- 8
standard deviation of speeds in tumor (m/s)	12	10	- 2
mean speed in surroundings (m/s)	1405	1407	+ 2
standard deviation of speeds in surroundings (m/s)	36	30	- 6

standard deviation of  $1.040 \text{ g/cm}^3$  and  $0.007 \text{ g/cm}^3$  with a reasonably symmetric distribution. The density distribution in the fatty surroundings is skewed as seen in the histogram, the dominant value being  $0.95 \text{ g/cm}^3$ , which is in the range of published values of  $0.93 \text{ g/cm}^3$  for pure fat and  $0.97 \text{ g/cm}^3$  for normal breast [8].

If one assumes that ultrasonic speed and density tend to increase and decrease together from one tissue to the next, then comparison of figures 5a or 5b with 5c indicates a high level of overlapping (registration) of density and

Table 2. Statistics for speed distributions shown in figures 6a and 6b.

	fresh specimen	fixed specimen (5% HCHO)	fixed value minus fresh value
mean speed in tumor (m/s)	1564	1570	+ 6
standard deviation of speeds in tumor (m/s)	12	12	0
mean speed in surroundings (m/s)	1440	1451	+ 11
standard deviation of speeds in surroundings (m/s)	21	21	0

MAPPING OF ULTRASONIC SPEED AND DENSITY

Table 3. Densities of fifteen 1 mm<sup>3</sup> pieces of tissue randomly selected from a fresh slice of breast tissue. Values are shown for the pieces when fresh (columns 1 and 3) and fixed for three days in 5% formaldehyde (columns 2 and 5). Changes - fixed minus fresh - are shown in columns 3 and 6.

densities (g/cm <sup>3</sup> )			change (g/cm <sup>3</sup> )	densities (g/cm <sup>3</sup> )			change (g/cm <sup>3</sup> )
fresh	fixed			fresh	fixed		
1.025	1.035	0.01		1.025	1.035	0.01	
1.03	1.045	0.015		1.03	1.045	0.015	
1.03	1.05	0.02		0.93	0.93	0	
0.93	0.94	0.01		1.04	1.055	0.015	
1.04	1.055	0.015		0.93	0.93	0	
0.98	0.99	0.01		1.03	1.05	0.02	
0.98	0.99	0.01		1.04	1.055	0.015	
1.03	1.045	0.015					

speed maps. A region of disagreement exists on the left of the map, about 1/3 up from the bottom. Higher densities are observed, but, except for a few pixels on the left side of this rectangular region, no elevation of speed was found. A thin extension from the carcinoma - perhaps 0.5 mm wide - of nonfatty tissue was observed visually in this region on one side of the 1 mm thick specimen before the density measurements were made.

For each of the ultrasonic speeds represented in figure 5a (fresh sample) there is a density at the corresponding pixel in figure 5c. A linear regression analysis of the set of approximately 400 corresponding pairs of speed and density values yielded a slope of  $3.798 \times 10^{-4}$  (g/cm<sup>3</sup>)/(m/s), a y intercept of 0.4430 g/cm<sup>3</sup> and a correlation coefficient [9] of 0.83. Thus, there is a strong correlation between ultrasonic speed and density.

In figure 5d is shown a mapping of acoustic impedances for the tissue slice. Each pixel value equals the product of the density and the ultrasonic speed (fresh sample) for the corresponding pixel in the density and speed maps.

Another diseased tissue on which measurements were made contained invasive scirrhous duct cell carcinoma from a 58 year old patient. Results for a tissue slice, a photograph of which is shown in figure 1, are shown in figures 6a through 6d and in table 2. In figure 6a is displayed the grey-scale ultrasonic speed distribution in this specimen obtained when the sample was fresh. The tumor occupies about 60% of the 20 mm by 20 mm scan field and corresponds to the light region of relatively uniform speeds in the upper left part of the map. The mean and standard deviation of the speeds in this tumor region are 1564 m/s and 12 m/s, respectively. The darker region on the lower right is fatty tissue with a mean speed of 1440 m/s and a standard deviation of 21 m/s.

In figure 6b is shown the map of ultrasonic speeds for this specimen after it had been stored for 1.5 days in normal saline containing 5% HCHO by weight. Note that this concentration is 5/2 that used for the sample mapped in figure 5. The mean speed and standard deviation in the tumor (upper left 60%) are 1570 m/s and 12 m/s, respectively, and in the remaining area are 1451 m/s and 21 m/s.

There are significant differences in the appearance of the speed maps for the fresh tissue (figure 6a) and the fixed tissue (figure 6b). Firstly, there is a region of lower speed in the lower left corner of figure 6b which is missing in figure 6a. Also, about 10 pixels forming the upper right corner in figure 6a are not uniform as in figure 6b. We surmise that a misalignment existed, shifting the center of 6b 3 mm to the right and 3 mm above that of figure 6a.

The means and standard deviations of the speeds in the tumor and in the region outside the tumor are shown in table 2 for measurements on the fresh sample and on the subsequently formalin-fixed sample. The mean values rose by less than 0.8% in both regions. However, the standard deviations did not change; thus, the mapping for the fixed specimen is likely as good as that for the fresh specimen as data for predicting local ultrasonic beam deviations or for guidance in phantom production.

In table 3 are shown densities of fifteen 1 mm<sup>3</sup> pieces of breast tissue when fresh and after fixing for three days in 5% formaldehyde; the fixing solution also contained 9 grams of NaCl per liter (normal saline concentration). The mean value of the change with fixing, for densities greater than 1.00 g/cm<sup>3</sup>, was 0.015 g/cm<sup>3</sup> and the corresponding standard deviation of the changes was 0.006 g/cm<sup>3</sup>. For densities less than 1.00 g/cm<sup>3</sup> the mean change was 0.004 g/cm<sup>3</sup> and the standard deviation was 0.006 g/cm<sup>3</sup>. The change for the lowest density pieces was essentially zero.

In figure 6c is the mapping of densities for the tissue sample corresponding to figures 6a and 6b. Assuming that an increase in speed tends to correspond to an increase in density for tissue, the density map and the speed map for the fixed tissue agree rather well. (The black pixels in figure 6c correspond to tissue pieces that were lost in the measurement process.)

Figure 7a shows a speed and 7b a density map for a series of 8 successive slices, labeled 1 through 8, through another duct cell carcinoma from a third patient. No formalin-fixing was done, density measurements being made immediately following speed measurements on each slice. All maps are approximately circular with diameters of about 18 mm, and the spacing between slices was actually 1.5 mm because a 0.5 mm thick slice was removed from between each of the 1 mm thick slices for histological analysis. The latter analysis showed that sections 1 through 4 consisted mostly of cancer with some fatty and fibrous tissue, and sections 5 through 8 were almost all carcinoma. The dark pixel in the lower central section of slice no. 1 corresponds to a received waveform having an amplitude of about 1/10 of the typical received waveforms; thus, the signal-to-noise ratio was very low and the speed value obtained for this pixel is not reliable. Histological analysis indicated that calcifications were present in this tissue, and it is possible that a larger calcification blocked most of the beam for this pixel.

Again assuming that increasing density corresponds to increasing ultrasonic speed, corresponding density and speed maps are generally consistent. Exceptions are on the upper left parts of slice 1 and the lower left part of slice 2. Histological analysis of adjacent 0.5 mm thick slices indicated that the upper left and lower left portions were fibro-fatty which might relate to the inconsistency. Regarding the assumption that increasing speed implies increasing density, it should also be kept in mind that longitudinal sound



## MAPPING OF ULTRASONIC SPEED AND DENSITY

speed is actually inversely proportional to the square root of the product of the density and compressibility. Thus, any generalization that sound speed in soft tissues always increases with density is not justified.

### VI. SUMMARY AND FURTHER DISCUSSION

A method has been described for measuring the distributions in ultrasonic speed and density over 1 mm thick slices of tissue with a resolution of about 1 mm. Speeds were measured at 37°C and densities at room temperature which was about 19°C. Accuracy of speed measurements was verified with a slice phantom composed of ultrasonically well characterized tissue-mimicking materials. The uncertainty in densities was estimated to be 0.006 g/cm<sup>3</sup> and the uncertainty in speeds has a minimum of 2 m/s at 1535 m/s, rising to 12 m/s at 1400 m/s and to 7 m/s at 1600 m/s; the variation in speed uncertainty relates almost entirely to the uncertainty in sample thickness. Measurements on diseased breast tissues from three different patients showed mean tumor speeds in the range of 1560 m/s with the mean speeds in the surroundings varying from about 1405 to 1450 m/s. Densities were found to increase with increasing speed, but when considerable fibrous tissue was mingled with fat, this rule did not apply. For a tissue slice in which registration between ultrasonic speed maps and the density map appeared to be within 1 mm, linear regression analysis showed good correlation between speed and density values. Evidence was found that measuring ultrasonic speed in tissue slices fixed in 5% formaldehyde and 0.9% NaCl is an acceptable alternative to using fresh tissues for producing acceptable tissue scattering models. The mean changes of speeds were + 0.8% in the surroundings and + 0.4% in the tumor, and the standard deviation in speeds inside and outside tumors was found to be invariant with 5% formaldehyde fixing. This was not true for measurements on samples fixed in 2% formaldehyde.

Changes in density with fixing in 5% formaldehyde were evaluated further for fifteen 1 mm<sup>3</sup> pieces of breast tissue. These changes ranged from zero in tissue of density 0.93 g/cm<sup>3</sup> to a mean of 0.015 g/cm<sup>3</sup> for samples with densities over 1.00 g/cm<sup>3</sup>. More extensive data comparing fixed with fresh densities as a function of density are being gathered in our laboratory. Perhaps a functional relation will be found between fixed and fresh densities so that measurement of fixed densities will suffice for estimating densities in the fresh state.

If measurements of speeds and densities on fixed tissues is found to be acceptable for specifying scattering models, this will make acquisition, via air freight, of usable tissue from hospitals throughout the country more convenient. Since appropriate diseased breast tissue is not readily available, such acquisitions could be important to our work regarding the compilation of an adequately large data base.

### VII. ACKNOWLEDGEMENTS

The authors gratefully acknowledge Prof. Mark Brownfield for the use of the cryostat and Thomas Bohlmann for helpful discussions. This work is supported in part by NIH grant R01 CA25634.

### APPENDIX

In this appendix, the derivatives in the expression for propagation of errors [eq. (2)] are evaluated, the uncertainty in the ultrasonic speed in the reference saline is then shown to be so small that it contributes negligibly to the uncertainty,  $\sigma$ , of the experimentally determined tissue ultrasonic speeds,

and, finally,  $\sigma$  is plotted versus  $c$ , the tissue ultrasonic speed, and approximate relative contributions to  $\sigma$  due to arrival time uncertainties ( $\sigma_t$  and  $\sigma_{t_0}$ ) and to sample thickness uncertainty  $\sigma_d$  are shown.

The derivatives in Eq. (2) are found using Eq. (1) yielding  $\partial c/\partial t = -\partial c/\partial t_0 = c^2/d$ ,  $\partial c/\partial d = c^2 \Delta t/d^2$ , and  $\partial c/\partial c_0 = c^2/c_0^2$ . Thus,

$$\sigma^2 = (c^4/d^2)[(\sigma_t^2 + \sigma_{t_0}^2) + (\Delta t/d)^2 \sigma_d^2 + d^2/(c^2 c_0^2) \sigma_{c_0}^2]. \quad (3)$$

From Eq. (1)  $(\Delta t/d)^2 = (c_0 - c)^2/(c_0 c)^2$ , and Eq. (3) becomes

$$\sigma^2 = (c^4/d^2)[(\sigma_t^2 + \sigma_{t_0}^2) + (c_0 - c)^2/(c_0^2 c^2) \sigma_d^2 + d^2/(c^2 c_0^2) \sigma_{c_0}^2]. \quad (4)$$

Next, consider the relative values of the first and third terms in brackets in Eq. (4). The first term has the value

$$\sigma_t^2 + \sigma_{t_0}^2 = 2(0.7 \times 10^{-9} \text{ s})^2 = 9.8 \times 10^{-19} \text{ s}^2,$$

and the third has an approximate upper bound of

$$d^2/(c_0 c)^2 \sigma_{c_0}^2 \approx [10^{-3} \text{ m}/(1400 \text{ m/s} \times 1535 \text{ m/s})]^2 \times (0.5 \text{ m/s})^2 = 5.4 \times 10^{-20} \text{ s}^2,$$

where  $c = 1400 \text{ m/s}$  was used. Comparing this value with the fixed value of  $\sigma_t^2 + \sigma_{t_0}^2$ , we see that the uncertainty in the saline speed,  $c_0$ , contributes negligibly to the uncertainty in  $c$  over the range of  $c$  involved.

The second term in brackets is a strong function of  $c_0 - c$ , going to zero at  $c = c_0$ . In figure 3 is shown a plot of  $\sigma$  versus  $c$  (solid line) and a plot of the contribution of  $\sigma$  due to the uncertainties,  $\sigma_t$  and  $\sigma_{t_0}$ , in arrival times only (dashed line). Approximate relative contributions to  $\sigma$  due to arrival time uncertainty and sample thickness uncertainty are apparent in the figure.

#### REFERENCES

- [1] Foster, F.S., Strban, M., and Austin, G., The ultrasound microscope: initial studies of breast tissue, Ultrasonic Imaging 6, 243-261 (1984).
- [2] Bamber, J.C., Bush, N., Quantitative mapping of acoustic and histological properties of excised tissue (abstr), J. Ultrasound Med. 7:S39-S283 (1988).
- [3] Madsen, E.L., Zagzebski, J.A., and Frank, G.R., Oil-in-gelatin dispersions for use as ultrasonically tissue-mimicking materials, Ultrasound Med. Biol. 8, 227-287 (1982).
- [4] LeCroy Corporation, The LeCroy Model 9400 Digital Oscilloscope Operators Manual (LeCroy Corporation, New York, 1986).
- [5] Greenleaf, J.F. and Bahn, R.C., Clinical imaging with transmissive ultrasonic computerized tomography, IEEE Trans. Biomed. Eng. BME-28, 177-185 (1981).

MAPPING OF ULTRASONIC SPEED AND DENSITY

- [6] Goss, S.A., Johnston, R.L., and Dunn, F., Comprehensive compilation of empirical ultrasonic properties of mammalian tissues, J. Acoust. Soc. Am. 64, 423-457 (1978).
- [7] Goss, S.A., Johnston, R.L., and Dunn, F., Compilation of empirical ultrasonic properties of mammalian tissues. II, J. Acoust. Soc. Am. 68, 93-108 (1980).
- [8] Rao, P.S. and Gregg, E.C., Am. J. Roentgenology 123, 631 (1975).
- [9] Sokolnikoff, I.S. and Redheffer, R.M. Mathematics of Physics and Modern Engineering (McGraw-Hill/New York, 1966) p. 641.